Article:
Foth, M, Ismail, NFB, Kung, JSC et al. (7 more authors) (2018) FGFR3 mutation increases bladder tumourigenesis by suppressing acute inflammation. Journal of Pathology, 246 (3). pp. 331-343. ISSN 0022-3417

https://doi.org/10.1002/path.5143

FGFR3 mutation increases bladder tumorigenesis by suppressing acute inflammation

Mona Foth[1, 2+], Nur Faezah Binti Ismail[1+], Jeng Sum Charmaine Kung[1], Darren Tomlinson[3], Margaret A. Knowles[3], Pontus Eriksson[4], Gottfrid Sjödahl[5], Jonathan M. Salmond[6], Owen J. Sansom[2,7] and Tomoko Iwata[1*]

[1]School of Medicine, Dentistry and Nursing, College of Medical, Veterinary and Life Sciences, University of Glasgow

[2]Cancer Research UK Beatson Institute, Glasgow, United Kingdom

[3]Leeds Institute of Cancer and Pathology, St James's University Hospital, Leeds, UK

[4]Division of Oncology and Pathology, Department of Clinical Sciences, Lund University, Lund, Sweden

[5]Division of Urological Research, Department of Translational Medicine, Lund University, Skåne University Hospital, Malmö, Sweden

[6]Department of Pathology, Queen Elizabeth University Hospital, Glasgow, United Kingdom

[7]Institute of Cancer Sciences, College of Medical, Veterinary and Life Sciences, University of Glasgow, United Kingdom

+These authors contributed equally to this manuscript

*Correspondence to: Tomoko Iwata, Medical Genetics and Pathology, Laboratory Medicine, Queen Elizabeth University Hospital, 1345 Govan Road, Glasgow, G51 4TF, United Kingdom

Phone: +44 141 354 9438. Email: Tomoko.Iwata@glasgow.ac.uk

No conflicts of interest were declared.

Running Title; Suppression of urothelial inflammation by FGFR3

This article has been accepted for publication and undergone full peer review but has not been through the copyediting, typesetting, pagination and proofreading process, which may lead to differences between this version and the Version of Record. Please cite this article as doi: 10.1002/path.5143

Abstract (224 words)

Recent studies of muscle-invasive bladder cancer show that FGFR3 mutations are generally found in a luminal papillary tumour subtype that is characterised by better survival than other molecular subtypes. To better understand the role of FGFR3 in invasive bladder cancer, we examined the process of tumour development induced by the tobacco carcinogen OH-BBN in genetically engineered models that express mutationally activated FGFR3 S249C or FGFR3 K644E in the urothelium. Both occurrence and progression of OH-BBN-driven tumours were increased in the presence of an S249C mutation compared to Wildtype control mice. Interestingly, at an early tumour initiation stage, the acute inflammatory response in OH-BBN-treated bladders was suppressed in the presence of an S249C mutation. However, at later stages of tumour progression, increased inflammation was observed in S249C tumours, long after the carcinogen administration had ceased. Early-phase neutrophil depletion using an anti-Ly6G monoclonal antibody resulted in an increased neutrophil-to-lymphocyte ratio at later stages of pathogenesis, indicative of enhanced tumour pathogenesis, which supports the hypothesis that suppression of acute inflammation could play a causative role. Statistical analyses of correlation showed that while initial bladder phenotypes in morphology and inflammation were FGFR3-dependent, increased levels of inflammation were associated with tumour progression at the later stage. This study provides a novel insight into the tumour-promoting effect of FGFR3 mutations via regulation of inflammation at the pre-tumour stage in the bladder.

Keywords: transitional cell carcinoma, transgenic mouse model, fibroblast growth factors, cancer immunology, neutrophils, inflammation, comparative pathology

Introduction

Bladder cancer is the 10th most common cancer type, particularly in aging men (Cancer Research UK, (http://www.cancerresearchuk.org/about-cancer/bladder-cancer/about, [accessed on 16/7/18]). The majority of bladder cancers are urothelial cell carcinoma (90%), followed by squamous cell carcinoma. Smoking is a major risk factor for bladder cancer. The majority of urothelial cell carcinoma at diagnosis is non-muscle invasive (NMIBC) (70%), the remainder showing muscle invasion. Muscle invasive bladder cancer (MIBC) without metastasis is managed by neoadjuvant chemotherapy followed by radical cystectomy [1]. However the recurrence rate is high, leading to local (10-15%) and distant (50%) metastasis.

Identifying effective therapies has been a challenge for bladder cancer clinically and pre-clinically, owing to a lack of full understanding of disease mechanisms [2]. However recent molecular analyses of large numbers of MIBC have defined several molecular subtypes and identified a range of potential therapeutic targets [3-7]. Abnormal immune regulation promotes tumour progression in many cancer types and could be an effective target for therapy [8]. Indeed, Bacillus Calmette-Guérin (BCG) immunotherapy is an effective adjuvant therapy for high-risk NMIBC that reduces disease recurrence and progression, and is offered as standard therapy [1]. More recently, clinical trials of inhibitors of immune checkpoint proteins, such as Programmed cell death protein 1 (PD-1) and PD ligand 1 (PD-L1), have shown success in advanced bladder cancer in terms of response rate and durability [2,9]. Nevertheless, reliable predictive biomarkers are lacking, and the role of acute and chronic inflammation and tumour immunity is still poorly understood in bladder cancer.

Fibroblast Growth Factor Receptor 3 (FGFR3) mutation and overexpression are common in bladder cancer [10-12]. According to the recent molecular classification of MIBC, tumours with

FGFR3 mutation and overexpression are associated with urothelial-like or luminal papillary tumour subgroups that are characterised by better survival than other molecular subtypes [7,13]. An activating point mutation in FGFR3 $^{C746C>G}$, encoding the FGFR3 S249C oncoprotein, accounts for 48-71% of all FGFR3 mutations in non-invasive urothelial cell carcinoma [14,15]. S249C affects the linker region between the extracellular immunoglobulin-like domains Ig2 and Ig3, which is important for the binding of FGF ligands. S249C triggers kinase activation through receptor dimerization as a result of disulphide bond formation in a completely ligand-independent manner [16]. In contrast, a lysine to glutamic acid substitution, K650E, in the kinase domain of FGFR3, found in a small number of bladder tumours (~1% of all mutations), exaggerates ligand-dependent kinase activation. Overexpression of wildtype FGFR3 receptor is found in 42% of muscle-invasive tumours [14]. An oncogenic fusion event of FGFR3 with the transforming acidic coiled-coil containing protein 3 (FGFR3-TACC3), leading to constitutive activation of FGFR3, is also found in bladder cancer [7,17,18].

FGFR3 is one of four tyrosine kinase receptors for FGFs [15,19]. In vitro studies have provided evidence that mutational activation of FGFR3 through S249C or K644E can modestly increase cell proliferation and reduce apoptosis, and that various FGFR inhibitors are effective in its functional suppression [19]. Current clinical trials are based on proof-of-principle studies in cell lines and xenograft models [20-24]. Phase II clinical trials of dovitinib, a multi-targeted RTK inhibitor that prevents phosphorylation of FGFR3, showed limited activity in advanced bladder cancer [25] and in BCG-unresponsive bladder cancer with mutations or overexpression of FGFR3 [26]. In contrast, a phase I trial of BGJ398 showed anti-tumour activity in FGFR3-mutated advanced bladder cancer after failure of platinum-based chemotherapy [27]. A phase I trial using an intermittent dosing schedule of the pan-FGFR3 inhibitor JNJ-42756493 on patients with advanced bladder cancer with confirmed FGFR alterations [28] and a case report

for phase I AZD4547, a selective FGFR inhibitor targeting FGFR1/2/3 [29] also showed promising results.

A better understanding of the role of FGFR3 mutations in tumour pathogenesis and progression will help in interpreting trial outcomes and allow further stratifications. The use of in vivo models closely reflecting the disease conditions would increase robustness and confidence in translation of pre-clinical findings to trials. Previously, we showed in a mouse model of spontaneous tumour formation that murine Fgfr3 K644E (equivalent to human K650E) in combination with Pten loss was able to induce morphological changes in the urothelium with cellular characteristics indicative of abnormal differentiation [30,31]. One of the most well-studied bladder carcinogens in mice is N-butyl-N-(4-hydroxybutyl)-nitrosamine (OH-BBN), derived from tobacco smoke [32]. OH-BBN induced tumours are of a highly invasive nature and often show a mixed histology with characteristics of both urothelial cell carcinoma and squamous cell differentiation. Similarities in histopathology and pathogenesis between the OH-BBN model and muscle-invasive bladder tumours in humans have been well established [33,34].

In this study, we have generated a novel transgenic mouse line that expresses FGFR3 S249C in the urothelium and compared the effects of OH-BBN to a Wildtype control, as well as to the previously reported Fgfr3 K644E model [30,31]. Furthermore, by neutrophil depletion, we have tested the hypothesis that impairment of acute inflammatory response at an early tumour initiation stage could promote tumour development.

Materials and methods

Mice: Generation of Tg(UroII-hFGFR3IIIbS249C) ("FGFR3^{S249C}") is described in supplementary material, Supplementary materials and methods. UroIICre Fgfr3$^{+/K644E}$ were

generated as previously described [31]. The Wildtype mice were C57Bl/6 (Charles River, Tranent, UK). Genetic background was C57Bl/6 in all cohorts.

Carcinogen treatment: Mice were administered 0.05% v/v OH-BBN (#B0938, TCI UK, Birkenhead, UK) in drinking water three times a week for 10 weeks, starting from 8-16 weeks of age, followed by 10 weeks of water. All experiments were performed according to an approved Project Licence under Home Office Animal (Scientific Procedures) Act 1986.

Neutrophil depletion: Wildtype mice were injected (i.p) with 500 μg of either 1A8 monoclonal antibody (anti-mLy-6G, Bioxcell, West Lebanon, NH, USA) or 2A3 isotype control (Rat IgG2a, Bioxcell) 3 times per week for 10 weeks, with concurrent OH-BBN administration in drinking water. Blood was collected in EDTA-containing tubes by cardiac puncture following euthanasia. White blood cell populations were analysed using ProCyte Dx Hematology Analyzer (IDEXX, Westbrook, ME, USA).

Histology and Immunohistochemistry (IHC): Methods and antibody details are provided in supplementary material, Supplementary materials and methods.

Scoring criteria: The number of mice showing the specific criterion was recorded, as assessed on one cross section per bladder. On the rare occasion that multiple lesions with different scoring criteria were present within one section, the more severe criterion was assigned.

Tumour phenotype; Stage of pathogenesis (minimal changes, urothelial hyperplasia or atypia, dysplastic urothelium or carcinoma in situ (CIS), tumour), "big" tumour, tumour size >50% of the bladder, "small" tumour, tumour size is <50% of the bladder; invasiveness (normal basement membrane, ambiguous basement membrane, breakage of basement membrane at multiple sites,

stromal invasion, muscle invasion, severe muscle invasion); lobulation of the basement membrane (none, mild or present locally, severe or multiple sites); squamous transformation (none, mild or small area, advanced, fully transformed and often keratinised). **Urothelial phenotype at 2 weeks**; atypia/dysplasia (minimal changes, atypia, dysplasia). **Inflammatory phenotype and neutrophils:** thickness of the stroma (normal, thickened, very thickened); angiogenesis in the inner stroma and in the outer stroma (normal, mild increase, notable increase). Neutrophil infiltrations at 2 and 12 weeks were scored in the urothelium, or stroma and muscle, using the criteria (<5, 6-20, 21-50, >50), where section size of the bladders were comparable among samples. Inflammatory phenotype at 20 weeks was scored using the criteria modified from Klintrup's method [35] (absent, presence of immune cells sparsely distributed, increase of immune cells clustering, very prominent inflammatory reaction).

Analysis of gene expression in TCGA cohorts and statistics: Details are provided in supplementary material, Supplementary materials and methods. The specific statistical method used is indicated in Figure legends. $P < 0.05$ was considered as statistically significant.

Results

Carcinogen-dependent tumorigenesis was increased in transgenic mice expressing mutationally-activated FGFR3 S249C.

In order to determine whether an S249C mutation in FGFR3 drives tumour pathogenesis in the bladder, we generated a transgenic mouse line that expresses the human FGFR3 IIIb isoform with an S249C mutation under control of the mouse uroplakin II promoter, Tg(UroII-hFGFR3IIIbS249C) ("FGFR3^{S249C}"). The histological appearance of the FGFR3^{S249C} urothelia (n=17) appeared normal at 12 months of age (Figure 1, spontaneous tumour formation, Table 1,

supplementary material, Figure S1). This was similar to observations in mice expressing the isogenic Fgfr3b-S249C transgene [36], as well as to heterozygous Fgfr3 K644E (UroIICre $Fgfr3^{+/K644E}$, "$Fgfr3^{K644E}$"), which we reported earlier [30,31], supporting that an FGFR3 mutation by itself is not able to induce urothelial pathogenesis. Furthermore, bladders of double mutant mice with both $FGFR3^{S249C}$ and Pten loss, "$FGFR3^{S249C}$ Pten" did not show any noticeable histological abnormalities at 12 months of age (n=12) (Table 1, supplementary material, Figure S1). This is in contrast to our previous observations in $Fgfr3^{K644E}$ Pten, which showed histopathological changes indicative of urothelial neoplasia [30,31].

Next, we used a carcinogen, OH-BBN, to induce invasive bladder cancer. Since bladder cancer is known to be more frequent in males than females in humans and in mice [37,38], we analysed the effects in both genders individually (the main Figures show the combined results from males/females. Results of individual genders are provided in the supplementary Figures, and are summarised in supplementary material, Table S1). At 20 weeks from the start of the carcinogen treatment, mice did not show any overt sign of adverse effects such as haematuria, although tumours in some animals were evident at dissection (Table 1). Metastases were not obvious in any of the cohorts. Subsequently, tumour pathogenesis in the bladder was evaluated histopathologically (Figure 2). Tumour pathogenesis in $FGFR3^{S249C}$ bladders was more advanced in contrast to Wildtype ($p=0.0454$) (Figure 2I). The invasive nature of the urothelial cells and the tumours was also increased in $FGFR3^{S249C}$ ($p=0.0239$) (Figure 2J). Carcinogen treatment caused the urothelium to show distinct characteristics, including a lobulated basement membrane (Figure 2E) and squamous transformation and keratinisation (Figure 2F). These features were also found to be increased in $FGFR3^{S249C}$ compared to Wildtype ($p=0.0073$ and <0.0001, respectively) (Figure 2K, L). $Fgfr3^{K644E}$ showed two cases of tumour formation (n=2/6 males) which invaded the stroma (Figure 2I).

Overall, the histopathology of carcinogen-induced tumours was more severe in the presence of an S249C mutation, indicating that both tumour occurrence and progression were enhanced. The phenotype of the $Fgfr3^{K644E}$ cohort was less severe than that of the $FGFR3^{S249C}$ mice, indicating that the two FGFR3 mutations are functionally distinct.

Differential time course of urothelial pathogenesis caused by the two FGFR3 mutations

We examined the bladder phenotype along the time course of carcinogen treatment (Figure 3, Table 1). Two weeks of OH-BBN treatment typically induced atypia and dysplasia and occasional hyperplasia of the urothelium (Figure 3A-C). Contrary to the phenotype at 20 weeks, these characteristics were reduced in the $FGFR3^{K644E}$ urothelia (n=10, comparing to Wildtype, n=17, p=0.0107) (Figure 3G).

At 12 weeks from the start of OH-BBN treatment, which included 10 weeks of OH-BBN dosing in drinking water and 2 weeks that followed without OH-BBN, the urothelium showed clearer characteristics of tumour pathogenesis, including carcinoma in situ (CIS) (Figure 3D-F). Lobulation of the basement membrane and squamous transformation was also apparent (Fig 3E, F). A statistically significant increase in urothelial pathogenesis and lobulation was found in $Fgfr3^{K644E}$ ($p = 0.0128$ and 0.0296, respectively) (Figure 3H, I).

Taken together, the increase in tumour pathogenesis became evident as early as 12 weeks from the start of the carcinogen treatment. Unexpectedly, at an early phase of carcinogen induction (2 week-time point), the histopathological changes in the urothelium were suppressed in the presence of FGFR3 K644E mutation, indicating differential regulation of urothelial pathogenesis by the two FGFR3 mutation.

Neutrophil infiltration was suppressed in FGFR3^{S249C} bladders upon carcinogen induction

In an attempt to understand the mechanisms that underlie tumour pathogenesis in FGFR3 mutant urothelium, we compared the effects of DNA damage caused by OH-BBN, by analysing the levels of γH2AX, p53, p21 and Ki67 (Fig S4), as well as indicators for signalling pathways, including phosphorylation of ERK, AKT, cJUN and STAT3 (data not shown). No alterations were found in DNA damage response and downstream signalling pathways in the FGFR3^{S249C} urothelium.

An acute inflammatory response caused by the administration of OH-BBN was apparent in the Wildtype bladders at 2 weeks (Figure 3K), in contrast to those not treated by OH-BBN (Figure 3J). The stroma of the OH-BBN-treated bladders was swollen and thickened, accompanied by small blood vessels forming at the inner stroma near the urothelium, and larger vessels were observed closer to the muscle. The overall inflamed appearance of the stroma, scored as stroma thickness and number of blood vessels, was similar between FGFR3 mutant and Wildtype cohorts (supplementary material, Figure S5A,B). Recruitment of neutrophils to the urothelium, the stroma, and to the muscle layer was clearly observed (Figure 3N), while effectively no neutrophils were observed in untreated bladders (Figure 3M). At 12 weeks from the start of OH-BBN treatment (2 weeks after the last carcinogen treatment), the stroma was typically less swollen than at 2 weeks (Figure 3L), however neutrophils remained to be frequently observed (Figure 3O).

Interestingly, by scoring the degree of neutrophil infiltration, suppression of neutrophil recruitment to the bladder became apparent in FGFR3^{S249C} compared to Wildtype mice at 2 weeks ($p=0.0466$, 0.0063, and 0.0464 in the urothelium, stroma, and muscle, respectively) (Figure 4A). Infiltration of F4/80^{+} macrophages was also assessed in FGFR3^{S249C}, indicating

that similar suppression may exist in the FGFR3^{S249C} urothelium (supplementary material, Figure S5C). At 12 weeks, neutrophil recruitment was no longer suppressed in FGFR3^{S249C} (Figure 4B). In contrast to 2 weeks, an increase in neutrophil infiltration was observed in Fgfr3^{K644E} stroma compared to Wildtype (p=0.0229) (Figure 4B).

We also investigated the status of tumour inflammation at 20 weeks. Interestingly, tumours were mildly more infiltrated by inflammatory cells in FGFR3^{S249C} compared to Wildtype (p=0.018) (Figure 4C). One of two Fgfr3^{K644E} tumours was highly infiltrated with neutrophils (score 3), while the other was not (score 0). The level of T-cell infiltration was similar in FGFR3^{S249C} and Wildtype tumours (supplementary material, Figure S7).

These results indicate that the acute inflammatory response to carcinogen treatment, particularly the recruitment of neutrophils to the bladder, was transiently suppressed in the presence of FGFR3 S249C mutation at the pre-tumour stage (2 weeks), while at 20 weeks, FGFR3^{S249C} bladders were mildly more inflamed than Wildtype.

Neutrophil depletion during pre-tumour stage resulted in increased inflammation

The early suppression of an acute inflammatory response could result in chronic inflammation later along the process of tumour progression, leading to enhanced tumour pathogenesis in the bladder. To investigate this, neutrophils were depleted using a monoclonal antibody against Ly-6G^{+} (1A8) along with OH-BBN treatment in a cohort of Wildtype mice [39] (Figure 5A). At 2 weeks of depletion, 1A8-treated mice showed significantly lower circulatory neutrophils in comparison with the isotype 2A3-treated control mice (Figure 5B). The neutrophils-to-lymphocyte ratio (NLR) in the blood was similarly reduced upon 1A8-treatment (Figure 5C). At

the tissue level, neutrophils were indicated to be effectively suppressed in the urothelium of 1A8-treated mice in comparison to 2A3-treated mice (supplementary material, Figure S8A).

Next, we sought to determine how neutrophil depletion during the pre-tumour stage would affect tumour progression. 1A8 was synchronously administered with OH-BBN for 10 weeks, and the levels of neutrophils were examined at 20 weeks. In contrast to the 2 weeks' time point, mice had a significantly higher NLR when previously treated with 1A8 ($p=0.0317$) (Figure 5E). Levels of neutrophil infiltration in the tumour tissue were comparable (Fig S8B). Interestingly, depletion of neutrophils during the pre-tumour stage indicated mildly more enhanced severity of tumour pathogenesis at 20 weeks (Figure 5F).

The results of the neutrophil depletion study indicated that the impairment of the acute inflammatory response at the pre-tumour stage could lead to a later increase in the levels of circulatory immune cells, indicative of enhanced progression of bladder tumours. This supports our hypothesis that the transient suppression of neutrophil recruitment to the bladder in FGFR3 S249C mice at the pre-tumour stage could account for increased tumorigenesis.

Early inflammatory phenotypes are associated with FGFR3 mutations, while late-phase inflammation is associated with tumour progression.

Changes in the levels of inflammatory infiltrations could be genotype-dependent (ie, changes in signalling by FGFR3 mutant proteins may have regulated the level of inflammation), or alternatively, phenotype-dependent (ie, inflammatory phenotype may have been caused by the severity of bladder/tumour pathology). In order to address this, we analysed the correlation between genotypes (cohort), phenotypes, and inflammation (supplementary material, Table S2-S4).

At 2 weeks, dysplasia significantly correlated with the cohort (Spearman's rank test rho: -0.405; p=0.007) (supplementary material, Table S2.1). The Kruskal-Wallis test showed that differences seen among cohorts were statistically significant in dysplasia (p=0.025), neutrophils in the stroma (p=0.003), and in the muscle (p=0.017) (supplementary material, Table S2.4), indicating that both dysplasia and inflammation were genotype-dependent.

At 12 weeks, cohort-dependent differences were evident in lobulation (rho: 0.435; p=0.021) and neutrophils in the stroma (rho: 0.435; p=0.022) (supplementary material, Table S3.1). Neutrophils in the stroma was also correlated with bladder phenotypes, including lobulation (rho: 0.671; p=0.00009), and squamous transformation (rho: 0.508; p=0.006). However, no statistically significant links were observed regarding neutrophils by the Kruskal-Wallis tests, either controlled by genotype (supplementary material, Table S3.4), or by pathogenesis (supplementary material, Table S3.7).

At 20 weeks, a positive correlation was evident in scores that indicate tumour pathogenesis (pathogenesis, invasiveness, lobulation and squamous transformation) and inflammation (overall inflammation in the urothelium, stroma, muscle and tumours) (supplementary material, Table S4.1). A significant correlation with cohort was seen in squamous transformation (rho: 0.323; p=0.002) (supplementary material, Table S4.1). Inflammation scores were notably correlated with those of pathogenesis. The Kruskal-Wallis test showed that inflammation in tumours was associated with pathogenesis (supplementary material, Table S4.7) and invasiveness (supplementary material, Table S4.10), however, no association was evident when controlled by cohort (supplementary material, Table S4.4).

Taken together, at an early phase of carcinogen induction, regulation of pathogenesis and inflammatory response was associated with the FGFR3 genotype, indicating the direct causative effects of the FGFR3 mutations. Once carcinogen treatment had ceased (12 weeks), inflammation was no longer regulated by FGFR3 mutations. At 20 weeks, only tumour pathogenesis was associated with FGFR3 genotype, and inflammation was associated with tumour progression.

In humans, tumours with FGFR3 mutation are associated with the urothelial-like or luminal papillary tumour subgroup that is generally characterised by lower levels of lymphocytic infiltration [7,13,40,41]. Here we stratified TCGA data [7] by FGFR3 mutation status and compared the immune gene expression signature [42]. In human MIBC, FGFR3 mutation did not influence the level of immune signature in any of the urothelial-like/luminal subtypes (supplementary material, Figure S9A,B). When subtypes were grouped together, human urothelial-like/luminal tumours with FGFR3 mutation were less immune-infiltrated than those with wild-type status (supplementary material, Figure S9C,D). However, this is due to the prevalence of Urothelial-like A-progressed (UroA-prog)/luminal-papillary subtypes that harbour FGFR3 mutations more frequently, and these subtypes were less immune infiltrated among the group regardless of FGFR3 mutation status (supplementary material, Figure S9A,B).

Discussion

By studying the effects of FGFR3 mutations using OH-BBN induced, genetically engineered mouse models of invasive bladder cancer, we report three significant findings: Firstly, in the presence of mutationally activated FGFR3 S249C, there was an increased number of mice that developed bladder tumours, and the tumour phenotype was more advanced (Figure 2). In $FGFR3^{S249C}$, tumour cells were more undifferentiated and invasive, with an increase in

squamous metaplasia. In the context of the skin, FGFR3 is expressed in keratinocytes, and FGFR3 mutation was associated with seborrheic keratosis [43]. Keratinisation in the mouse model in this study can be interpreted as an advanced feature of tumour progression. Secondly, the inflammatory response was unexpectedly suppressed in the presence of an S249C mutation at an early time of carcinogen induction (Figure 4). Acute inflammation is associated with an anti-tumour response [8]. A reduced clearance of DNA-damaged cells may have led to overall increased tumour formation in $FGFR3^{S249C}$ at later stages (proposed in Figure 6). Although involvement of FGF signalling has been reported in inflammatory diseases and in the tumour microenvironment [44], the mechanisms that underlie early suppression of inflammatory response by S249C-mutated FGFR3 are currently unknown. FGFR3 is not expressed in neutrophils [45]. FGFR3 mutations are not associated with smoking [46], and are not found in OH-BBN-induced tumours in mice [47]. Studies on genomic and transcriptional profiles of the tumour samples generated in this study may be useful in order to gain further mechanistic insights into the suppression of acute inflammation and tumorigenesis in the presence of FGFR3 mutations. Thirdly, established tumours in $FGFR3^{S249C}$ were mildly more inflamed compared to Wildtype tumours (Figure 4). This increase in inflammation was mainly associated with overall tumour progression, rather than FGFR3 mutations (supplementary material, Table S4). No significant differences were observed in the levels of T-cells (supplementary material, Figure S7). Neutrophil depletion at an early phase increased the NLR later at 20 weeks, during the timeframe of tumour establishment and progression, indicative of enhanced tumour pathogenesis (Figure 5). A high circulatory NLR is generally associated with poor prognosis, including in bladder cancer [48-51]. However, the level of neutrophils in the tumours remained similar regardless of early depletion (supplementary material, Figure S8). Therefore, effects of immune microenvironment on tumour progression are not expected in this model (Figure 5F). Whether suppression of acute inflammatory response leads to tumour inflammation, and whether such inflammation reciprocally enhances tumour progression, remain unresolved.

FGFR3 mutations are commonly found in urothelial-like/luminal papillary tumour subtypes generally associated with better prognosis, and accompanied by low levels of lymphocytic infiltration [7,13,40,41]. In the context of PD-1/PD-L1 checkpoint blockade therapy, presence of T-cell populations was shown to be an important indicator for the patients' response, where low levels of $CD3^+$ and $CD8^+$ T-cells are associated with poor outcome [9,51,52]. It has been reported recently that FGFR3 mutations are frequently found in non-$CD8^+$ T-cell-inflamed MIBC, and it was proposed that FGFR3 pathway could be targeted to overcome resistance and sensitise tumours to PD-1/PD-L1 immunotherapy [40]. Our analysis of urothelial-like/luminary papillary tumour subtypes in the TCGA dataset showed that the expression of immune genes was not affected by the presence or absence of FGFR3 mutations in each of the different subtypes of the Lund or TCGA classification (supplementary material, Figure S9). This included the Urothelial-like B (UroB), a subtype with the worst overall survival, similar to Small-cell/Neuroendocrine-like (Sc/NE-like) [13]. Lower infiltration was indeed associated with FGFR3 mutation when all subtypes within urothelial-like/luminary papillary subtypes were combined, however, this is due to frequency of lower-infiltrated subgroups, such as UroA-Prog/Luminal-papillary subtypes (supplementary material, Figure S9C,D). The lack of difference in immune gene expression within the tumour subtype in the presence and absence of FGFR3 mutation in human MIBC could be due to the fact that human studies are based on established tumours, while our study in mouse models investigates the functional effects of FGFR3 along the process of tumour initiation and development, the earlier phases in tumour pathogenesis. It would be interesting to compare the levels of tumour inflammation in OH-BBN-induced bladder models with other molecular changes, such as Tp53, Stat3 and Sparc models [53]. To facilitate the evaluation, we have previously generated the "Tumour Progression Scale" in phenotyping mouse bladder tumours with an inflammatory phenotype [54].

Examining the individual FGFR3 mutations, early suppression of neutrophil infiltration was not present in the $Fgfr3^{K644E}$ (Figure 4). Instead, an increase in pathogenesis was observed at 2 weeks and 12 weeks (Figure 3) and stromal neutrophil infiltration was increased in $Fgfr3^{K644E}$ (Figure 4B), indicating earlier kinetics in urothelial pathogenesis. Nonetheless, it did not lead to a significant increase in tumorigenesis at the 20-week endpoint (Figure 2). Therefore, the effects of individual FGFR3 mutations in regulating neutrophils and tumour pathogenesis are distinct, and may explain the low frequency of kinase domain mutations in human bladder neoplasia. Mechanistically, the way these two mutations regulate the receptor protein kinase function and downstream signalling could be different [15,16]. For example, S249C leads to phosphorylation of PLCγ1, while the equivalent kinase domain mutation K652E does not [55]. The cell-cell and cell-matrix adhesion were also indicated to be differently regulated in cells expressing S249C and K652E [56]. Effects of gender in bladder cancer epidemiology and underlying mechanism are well discussed [37,38]. The results of male/female combined analyses were consistent with those done individually (summarised in supplementary material, Table S1). However, a small number of mice used may have masked any effects.

In summary, our study showed that the increased tumour progression could be initiated by the effects of FGFR3 mutations in regulating an acute inflammatory response, and that immune cells are perturbed in the tumour as a consequence. Clinically, it would be beneficial to explore FGFR3 inhibition together with the concurrent immune modulators, such as BCG, as a potential treatment strategy for FGFR3-mutated or -overexpressing bladder cancer at an early stage.

Acknowledgements

This work was funded by University of Glasgow MRC Centenary Award (MF), JPA Public Service Department of Malaysia (NFBI), Pathological Society of Great Britain and Ireland,

Wellcome Trust (JSCK), Beatson Endowment Fund (JMS) and Cancer Research UK A21139, A12481 and A17196 (OJS). We would like to thank staffs of Histology Services at the CRUK Beatson Institute for their technical support.

Author contributions

MF, NFBI, JSCK and TI performed experiments and analysed the results, DT, MK designed and generated FGFR3^{S249C} transgene vector, PE and GS performed bioinformatic evaluation of the role of FGFR3 mutation in Lund/TCGA cohorts, JMS advised on histopathology, MF, NFBI, JSCK and TI wrote the manuscript, OJS and TI supervised the overall project. All authors edited the draft manuscript.

References

1. Alfred Witjes J, Lebret T, Comperat EM, et al. Updated 2016 EAU Guidelines on Muscle-invasive and Metastatic Bladder Cancer. Eur Urol 2017; **71:** 462–475.
2. Kurtoglu M, Davarpanah NN, Qin R, et al. Elevating the horizon: emerging molecular and genomic targets in the treatment of advanced urothelial carcinoma. Clin Genitourin Cancer 2015; **13:** 410–420.
3. Sjodahl G, Lauss M, Lovgren K, et al. A molecular taxonomy for urothelial carcinoma. Clin Cancer Res 2012; **18:** 3377–3386.
4. Guo G, Sun X, Chen C, et al. Whole-genome and whole-exome sequencing of bladder cancer identifies frequent alterations in genes involved in sister chromatid cohesion and segregation. Nat Genet 2013; **45:** 1459–1463.
5. Damrauer JS, Hoadley KA, Chism DD, et al. Intrinsic subtypes of high-grade bladder cancer reflect the hallmarks of breast cancer biology. Proc Natl Acad Sci U S A 2014; **111:** 3110–3115.
6. Choi W, Porten S, Kim S, et al. Identification of distinct basal and luminal subtypes of muscle-invasive bladder cancer with different sensitivities to frontline chemotherapy. Cancer Cell 2014; **25:** 152–165.
7. Robertson AG, Kim J, Al-Ahmadie H, et al. Comprehensive molecular characterization of muscle-invasive bladder cancer. Cell 2017; **171:** 540–556 e25.
8. Schreiber RD, Old LJ, Smyth MJ. Cancer immunoediting: integrating immunity's roles in cancer suppression and promotion. Science 2011; **331:** 1565–1570.
9. Carosella ED, Ploussard G, LeMaoult J, et al. A systematic review of immunotherapy in urologic cancer: evolving roles for targeting of CTLA-4, PD-1/PD-L1, and HLA-G. Eur Urol 2015; **68:** 267–279.
10. Guancial EA, Werner L, Bellmunt J, et al. FGFR3 expression in primary and metastatic urothelial carcinoma of the bladder. Cancer Med 2014; **3:** 835–844.

11. Pouessel D, Neuzillet Y, Mertens LS, et al. Tumor heterogeneity of fibroblast growth factor receptor 3 (FGFR3) mutations in invasive bladder cancer: implications for perioperative anti-FGFR3 treatment. Ann Oncol 2016; **27:** 1311–1316.
12. Glaser AP, Fantini D, Shilatifard A, et al. The evolving genomic landscape of urothelial carcinoma. Nat Rev Urol 2017; **14:** 215–229.
13. Marzouka NA, Eriksson P, Rovira C, et al. A validation and extended description of the Lund taxonomy for urothelial carcinoma using the TCGA cohort. Sci Rep 2018; **8:** 3737.
14. Tomlinson DC, Baldo O, Harnden P, et al. FGFR3 protein expression and its relationship to mutation status and prognostic variables in bladder cancer. J Pathol 2007; **213:** 91–98.
15. Ahmad I, Iwata T, Leung HY. Mechanisms of FGFR-mediated carcinogenesis. Biochim Biophys Acta 2012; **1823:** 850–860.
16. Naski MC, Wang Q, Xu J, et al. Graded activation of fibroblast growth factor receptor 3 by mutations causing achondroplasia and thanatophoric dysplasia. Nat Genet 1996; **13:** 233–237.
17. Williams SV, Hurst CD, Knowles MA. Oncogenic FGFR3 gene fusions in bladder cancer. Hum Mol Genet 2013; **22:** 795–803.
18. Cancer Genome Atlas Research Network. Comprehensive molecular characterization of urothelial bladder carcinoma. Nature 2014; **507:** 315–322.
19. Babina IS, Turner NC. Advances and challenges in targeting FGFR signalling in cancer. Nat Rev Cancer 2017; **17:** 318–332.
20. Qing J, Du X, Chen Y, et al. Antibody-based targeting of FGFR3 in bladder carcinoma and t(4;14)-positive multiple myeloma in mice. J Clin Invest 2009; **119:** 1216–1229.
21. Lamont FR, Tomlinson DC, Cooper PA, et al. Small molecule FGF receptor inhibitors block FGFR-dependent urothelial carcinoma growth in vitro and in vivo. Br J Cancer 2011; **104:** 75–82.

22. Guagnano V, Furet P, Spanka C, et al. Discovery of 3-(2,6-dichloro-3,5-dimethoxy-phenyl)-1-{6-[4-(4-ethyl-piperazin-1-yl)-phenylamin o]-pyrimidin-4-yl}-1-methyl-urea (NVP-BGJ398), a potent and selective inhibitor of the fibroblast growth factor receptor family of receptor tyrosine kinase. J Med Chem 2011; **54:** 7066–7083.
23. Gavine PR, Mooney L, Kilgour E, et al. AZD4547: an orally bioavailable, potent, and selective inhibitor of the fibroblast growth factor receptor tyrosine kinase family. Cancer Res 2012; **72:** 2045–2056.
24. Gust KM, McConkey DJ, Awrey S, et al. Fibroblast growth factor receptor 3 is a rational therapeutic target in bladder cancer. Mol Cancer Ther 2013; **12:** 1245–1254.
25. Milowsky MI, Dittrich C, Duran I, et al. Phase 2 trial of dovitinib in patients with progressive FGFR3-mutated or FGFR3 wild-type advanced urothelial carcinoma. Eur J Cancer 2014; **50:** 3145–3152.
26. Hahn NM, Bivalacqua TJ, Ross AE, et al. A phase II trial of dovitinib in BCG-unresponsive urothelial carcinoma with FGFR3 mutations or overexpression: Hoosier Cancer Research Network Trial HCRN 12-157. Clin Cancer Res 2017; **23:** 3003–3011.
27. Nogova L, Sequist LV, Perez Garcia JM, et al. Evaluation of BGJ398, a fibroblast growth factor receptor 1-3 kinase inhibitor, in patients with advanced solid tumors harboring genetic alterations in fibroblast growth factor receptors: results of a global phase I, dose-escalation and dose-expansion study. J Clin Oncol 2017; **35:** 157–165.
28. Tabernero J, Bahleda R, Dienstmann R, et al. Phase I dose-escalation study of JNJ-42756493, an oral pan-fibroblast growth factor receptor inhibitor, in patients with advanced solid tumors. J Clin Oncol 2015; **33:** 3401–3408.
29. Rodriguez-Vida A, Saggese M, Hughes S, et al. Complexity of FGFR signalling in metastatic urothelial cancer. J Hematol Oncol 2015; **8:** 119.

30. Ahmad I, Singh LB, Foth M, et al. K-Ras and beta-catenin mutations cooperate with Fgfr3 mutations in mice to promote tumorigenesis in the skin and lung, but not in the bladder. Dis Model Mech 2011; **4:** 548–555.
31. Foth M, Ahmad I, van Rhijn BW, et al. Fibroblast growth factor receptor 3 activation plays a causative role in urothelial cancer pathogenesis in cooperation with Pten loss in mice. J Pathol 2014; **233:** 148–158.
32. Vasconcelos-Nobrega C, Colaco A, Lopes C, et al. Review: BBN as an urothelial carcinogen. In Vivo 2012; **26:** 727–739.
33. Shin K, Lim A, Odegaard JI, et al. Cellular origin of bladder neoplasia and tissue dynamics of its progression to invasive carcinoma. Nat Cell Biol 2014; **16:** 469–478.
34. Van Batavia J, Yamany T, Molotkov A, et al. Bladder cancers arise from distinct urothelial sub-populations. Nat Cell Biol 2014; **16:** 982–991, 981–985.
35. Klintrup K, Makinen JM, Kauppila S, et al. Inflammation and prognosis in colorectal cancer. Eur J Cancer 2005; **41:** 2645–2654.
36. Zhou S, Xie Y, Li W, et al. Conditional deletion of Fgfr3 in chondrocytes leads to osteoarthritis-like defects in temporomandibular joint of adult mice. Sci Rep 2016; **6:** 24039.
37. Miyamoto H, Yang Z, Chen YT, et al. Promotion of bladder cancer development and progression by androgen receptor signals. J Natl Cancer Inst 2007; **99:** 558–568.
38. Lucca I, Klatte T, Fajkovic H, et al. Gender differences in incidence and outcomes of urothelial and kidney cancer. Nat Rev Urol 2015; **12:** 585–592.
39. Jamieson T, Clarke M, Steele CW, et al. Inhibition of CXCR2 profoundly suppresses inflammation-driven and spontaneous tumorigenesis. J Clin Invest 2012; **122:** 3127–3144.
40. Sweis RF, Spranger S, Bao R, et al. Molecular drivers of the non-T-cell-inflamed tumor microenvironment in urothelial bladder cancer. Cancer Immunol Res 2016; **4:** 563–568.

41. Kilgour E, Angell H, Smith NR, et al. Fibroblast growth factor receptor 3 (FGFR3) mutant muscle invasive bladder cancers (MIBC) are associated with low immune infiltrates. Ann Oncol 2016; **27:** 786P–786P.
42. Yoshihara K, Shahmoradgoli M, Martinez E, et al. Inferring tumour purity and stromal and immune cell admixture from expression data. Nat Commun 2013; **4:** 2612.
43. Hafner C, Hartmann A, Vogt T. FGFR3 mutations in epidermal nevi and seborrheic keratoses: lessons from urothelium and skin. J Invest Dermatol 2007; **127:** 1572–1573.
44. Presta M, Chiodelli P, Giacomini A, et al. Fibroblast growth factors (FGFs) in cancer: FGF traps as a new therapeutic approach. Pharmacol Ther 2017; **179:** 171–187.
45. Haddad LE, Khzam LB, Hajjar F, et al. Characterization of FGF receptor expression in human neutrophils and their contribution to chemotaxis. Am J Physiol Cell Physiol 2011; **301:** C1036–1045.
46. Wallerand H, Bakkar AA, de Medina SG, et al. Mutations in TP53, but not FGFR3, in urothelial cell carcinoma of the bladder are influenced by smoking: contribution of exogenous versus endogenous carcinogens. Carcinogenesis 2005; **26:** 177–184.
47. Dunois-Larde C, Levrel O, Brams A, et al. Absence of FGFR3 mutations in urinary bladder tumours of rats and mice treated with N-butyl-N-(-4-hydroxybutyl)nitrosamine. Mol Carcinog 2005; **42:** 142–149.
48. Coffelt SB, Wellenstein MD, de Visser KE. Neutrophils in cancer: neutral no more. Nat Rev Cancer 2016; **16:** 431–446.
49. Templeton AJ, McNamara MG, Seruga B, et al. Prognostic role of neutrophil-to-lymphocyte ratio in solid tumors: a systematic review and meta-analysis. J Natl Cancer Inst 2014; **106:** dju124.
50. Gentles AJ, Newman AM, Liu CL, et al. The prognostic landscape of genes and infiltrating immune cells across human cancers. Nat Med 2015; **21:** 938–945.

51. Masson-Lecomte A, Rava M, Real FX, et al. Inflammatory biomarkers and bladder cancer prognosis: a systematic review. Eur Urol 2014; **66:** 1078–1091.
52. Sweis RF, Galsky MD. Emerging role of immunotherapy in urothelial carcinoma-Immunobiology/biomarkers. Urol Oncol 2016; **34:** 556–565.
53. Ahmad I, Sansom OJ, Leung HY. Exploring molecular genetics of bladder cancer: lessons learned from mouse models. Dis Model Mech 2012.
54. Kung CJS, Kiourtis C, Fraser S, et al. Establishment of Tumour Progression Scale for Invasive Bladder Cancer Models. Abstracts of the 205th Meeting of the Pathological Society of Great Britain & Ireland. J Pathol 2016; **238:** S1–S20.
55. di Martino E, L'Hote CG, Kennedy W, et al. Mutant fibroblast growth factor receptor 3 induces intracellular signaling and cellular transformation in a cell type- and mutation-specific manner. Oncogene 2009; **28:** 4306–4316.
56. di Martino E, Kelly G, Roulson JA, et al. Alteration of cell-cell and cell-matrix adhesion in urothelial cells: an oncogenic mechanism for mutant FGFR3. Mol Cancer Res 2015; **13:** 138–148.
57. Mo L, Cheng J, Lee EY, et al. Gene deletion in urothelium by specific expression of Cre recombinase. Am J Physiol Renal Physiol 2005; **289:** F562–568.
58. Lesche R, Groszer M, Gao J, et al. Cre/loxP-mediated inactivation of the murine Pten tumor suppressor gene. Genesis 2002; **32:** 148–149.

Table 1. Summary of the mouse cohorts

Models of spontaneous tumour formation			
Genotype	**Age at time of analysis**	**Cohort size (n) Male (m) Female (f)**	**Gross observation at time point**
Control	10-18 months	11 (m = 1; f =10)	None
$FGFR3^{S249C}$	6-12 months	17 (m =10; f = 7)	Non-bladder related death in n=2 (12%)
$FGFR3^{S249C}$Pten	12 months	12 (m = 6; f = 6)	Non-bladder related death in n=1 (8%)
Carcinogen-induced bladder cancer model			
Genotype	**OH-BBN treatment (weeks)**	**Cohort size (n) Male (m) Female (f)**	**Gross observation at time point**
Wild type	2	17 (m=8; f=9)	None
	12	10 (m=3; f=7)	None
	20	47 (m=20; f=27)	Tumour (m=5; f=1)
$FGFR3^{S249C}$	2	15 (m=10; f=5)	None
	12	10 (m=3; f=7)	None
	20	29 (m=12; f=17)	Tumour (m=3; f=6)
$FGFR3^{K644E}$	2	11 (m=4; f=7)	None

12	8 (m=3; f=5)	None
20	11 (m=6; f=5)	Tumour (m=2; f=0)

The Tg(UroII-hFGFR3IIIbS249C) mouse line ($FGFR3^{S249C}$) was generated as described in Supplementary Methods. UroIICre [57], $Pten^{flox/flox}$ [58] were intercrossed with $FGFR3^{S249C}$ to generate $FGFR3^{S249C}$ $Pten^{flox/flox}$ mice ($FGFR3^{S249C}$ Pten). The Controls were C57Bl/6 (Charles River, UK) ("Wildtype") (n=7) and mice with transgenic alleles which do not lead to any phenotype (n=4). Genetic background was C57Bl/6 in all cohorts. For carcinogen induction, mice at 8-16 weeks of age were administered with 0.05% (v/v) OH-BBN in drinking water for 10 weeks followed by 10 weeks of normal drinking water. Mice used were Wildtype, $FGFR3^{S249C}$ and UroIICre $Fgfr3^{+/K644E}$ ($FGFR3^{K644E}$) [31].

Figure legends

Figure 1. Schematic presentation of the mouse cohorts studied and timeline of carcinogen induction. The role of FGFR3 mutations was investigated using models of spontaneous tumour formation (left). FGFR3 mutation by itself, either K644E [30,31] or S249C (this study), did not lead to urothelial pathogenesis. While double mutant mice $Fgfr3^{K644E}$ Pten resulted in histopathological abnormalities [31], $FGFR3^{S249C}$ Pten bladders did not show any noticeable histological changes at 12 months. For carcinogen-induced model of invasive bladder tumours (right), tobacco carcinogen, OH-BBN. 0.05% (v/v) OH-BBN was administered to mice in drinking water for the first 10 weeks, then tumours were allowed to develop for a further 10 weeks. The histopathology of the bladders and tumours was examined at 2, 12 and 20 week time points.

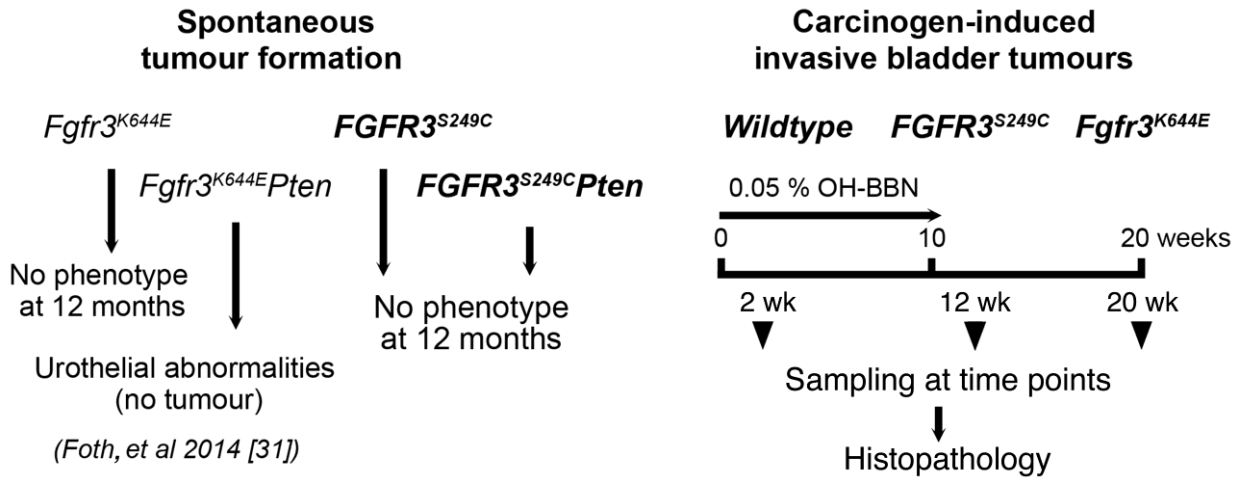

Figure 2. Histopathology of the urothelium and bladder tumours at 20 weeks from the start of carcinogen treatment.

Representative images of minimal changes (**A**), hyperplasia (**B**), dysplasia (**C**), carcinoma in situ (CIS) (**D**). The basement membrane was often lobulated (**E**) and the urothelium was squamous transformed with keratinised surfaces (arrowhead) (**F**). An additional examples of CIS (red arrowhead) is indicated in examples of fully developed tumours (**G, H**) with stromal invasion (black arrowhead) (**G**). The leading edge of the invading tumour was often infiltrated with inflammatory cells (arrowhead in **H**). Scale bar represents 50 µm in **A,B,E**, 70 µm in C, 100 µm in D, 125 µm in **F**, 500 µm in **G** and 700 µm in **H**. (**I-L**) The observed phenotype was shown as percentage of mice that showed the specific phenotypic criterion. (**I**) Pathogenesis observed in the bladder. (**J**) Invasiveness of the urothelial and tumour cells. (**K**) Lobulated appearance of the basement membrane. (**L**) Squamous differentiation observed in the urothelium and the tumour. In **I-L**, Number of samples analysed was n=47, 29, and 11, for Wildtype, $FGFR3^{S249C}$ and $Fgfr3^{K644E}$, respectively (results for males and females combined are shown here). The p-values (Mann-Whitney) are indicated above the columns, when significant (*<0.05 and **< 0.005).

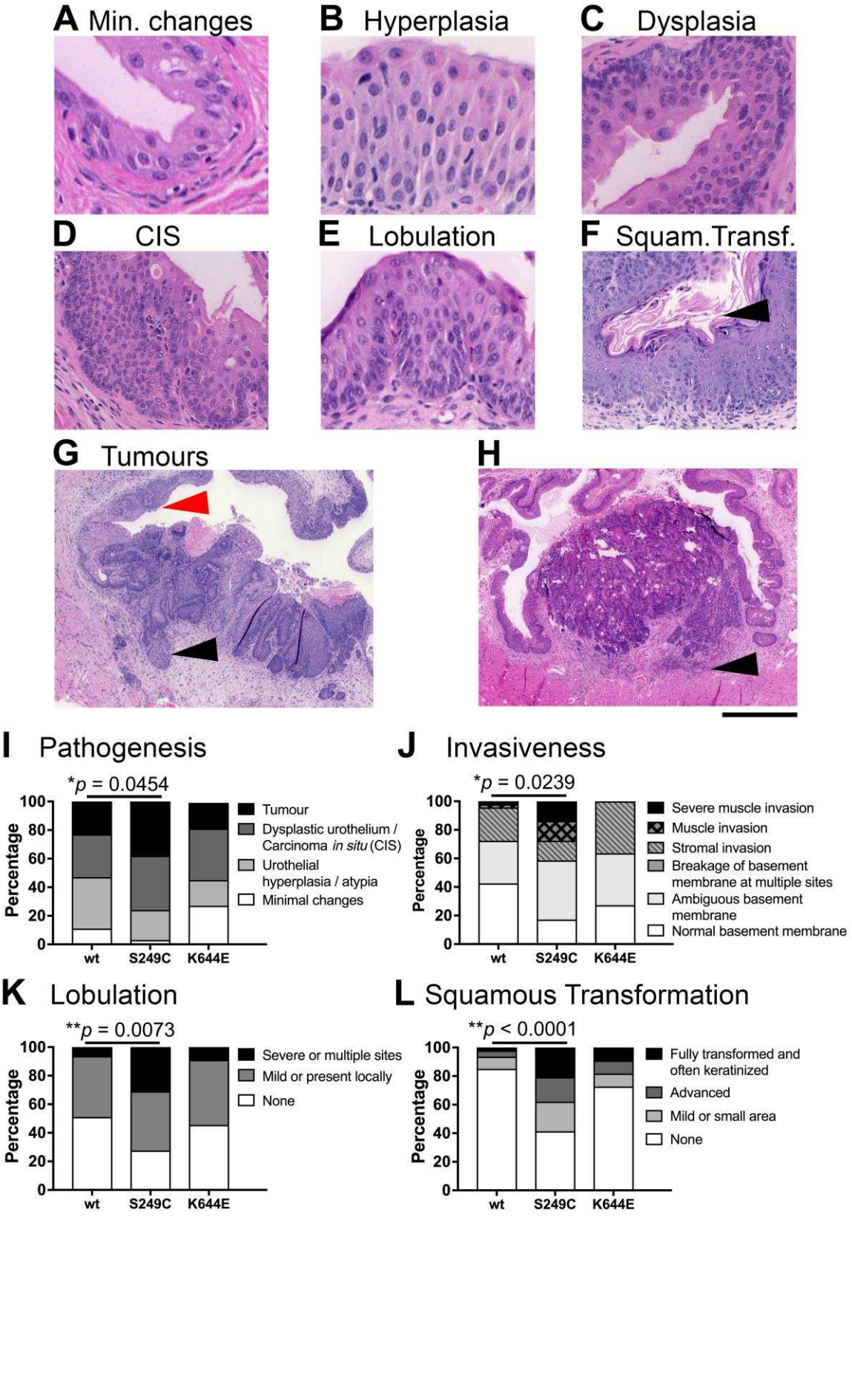

Figure 3. Histopathological and inflammatory phenotype of the bladder at 2 and 12 weeks from the start of carcinogen treatment.

Representative H&E images of the urothelium of Wildtype (**A, D**), $FGFR3^{S249C}$ (**B, E**) and $Fgfr3^{K644E}$ (**C, F**) at 2 (**A-C**) and 12 weeks (**D-F**) from the start of OH-BBN treatment. Lobulated basement membrane (arrowheads in **E**) and squamous transformation (arrowheads in **F**) was visible at 12 weeks. (**G**) Presence of atypia and dysplasia in the urothelium at 2 weeks was scored in n=17, 15, and 10 samples of Wildtype, $FGFR3^{S249C}$ and $Fgfr3^{K644E}$, respectively. Pathogenesis (**H**) and lobulation of the basement membrane (**I**) at 12 weeks were scored in n=10, 10, and 8 samples of Wildtype, $FGFR3^{S249C}$ and $Fgfr3^{K644E,}$ respectively. The Y-axis indicates percentage of mice that showed the specific phenotypic criterion. The p-values (Mann-Whitney) are indicated when significant (*<0.05). In the absence of OH-BBN, no sign of inflammation was present, and no neutrophils were observed (**J, M**). In contrast, 2 weeks of carcinogen treatment caused the bladder to be inflamed with thickened stroma with inner and outer bands (**K**), with increased presence of neutrophils in the urothelium and in the stroma (arrowheads in **N**). At 12 weeks from the start of the carcinogen treatment (2 weeks after mice had been returned to the normal drinking water), the bladders showed a mixture of inflamed and normal areas (**L**). Neutrophils were also observed at 12 weeks (arrowheads) (**O**). Scale bar represents 100 µm in **A-F**, 300 µm in **J, K**, 500 µm in **L**, 50 µm in **M-O**.

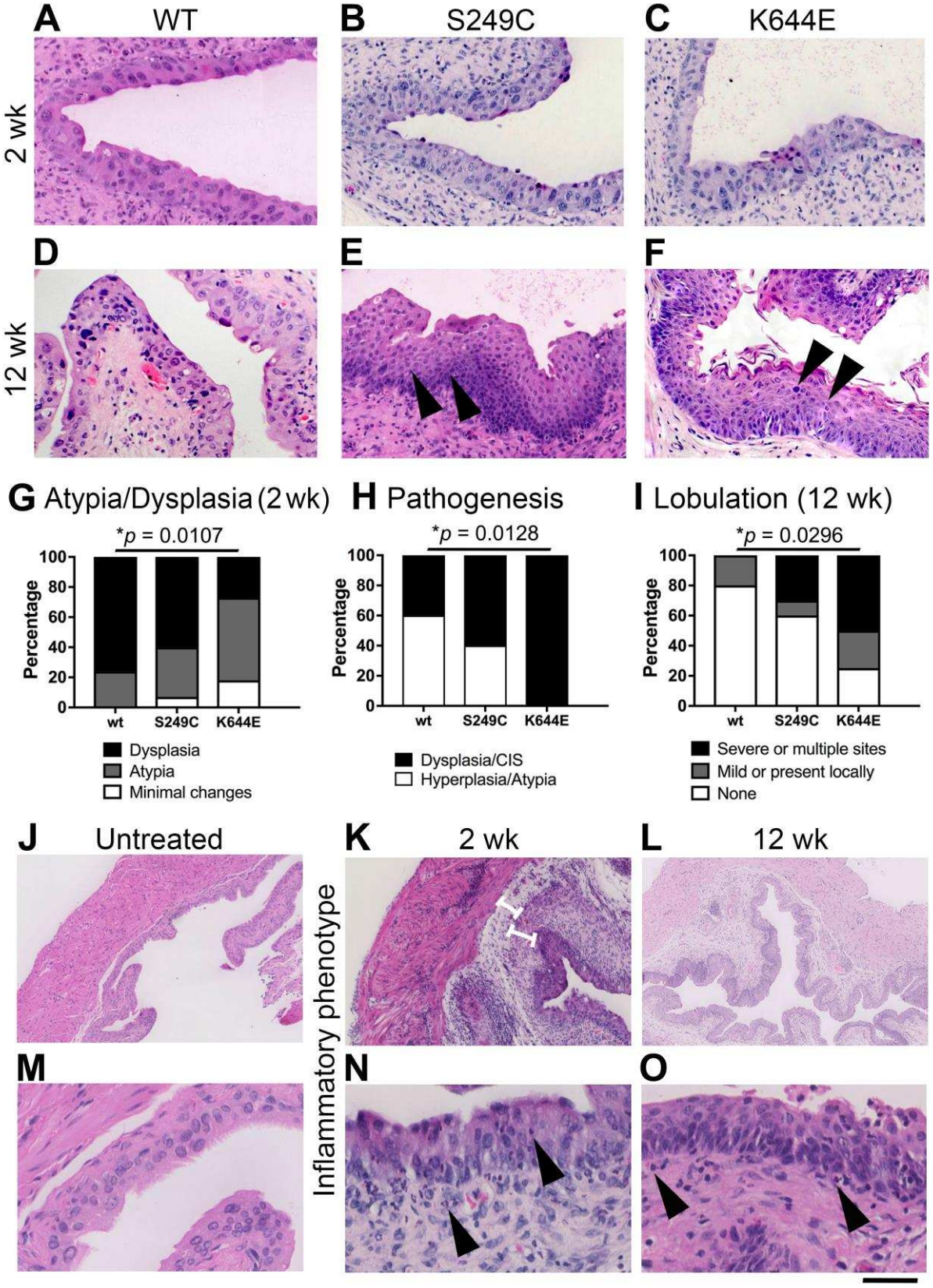

Figure 4. Infiltration of neutrophils in the bladder and bladder tumours at time points of carcinogen treatment.

Presence of neutrophils in the urothelium, stroma**,** and muscle layer of the bladder at 2 weeks (**A**) and 12 weeks (**B**) from the start of OH-BBN treatment. (**C**) The status of overall inflammation (left**)** and infiltration of neutrophils **(**right) in the tumours observed at 20 weeks from the start of OH-BBN treatment. The Y-axis indicates percentage of mice that showed the specific phenotypic criterion. Number of samples analysed is indicated below each column. The p-values (Mann-Whitney) are indicated where significant (*<0.05 and **< 0.005).

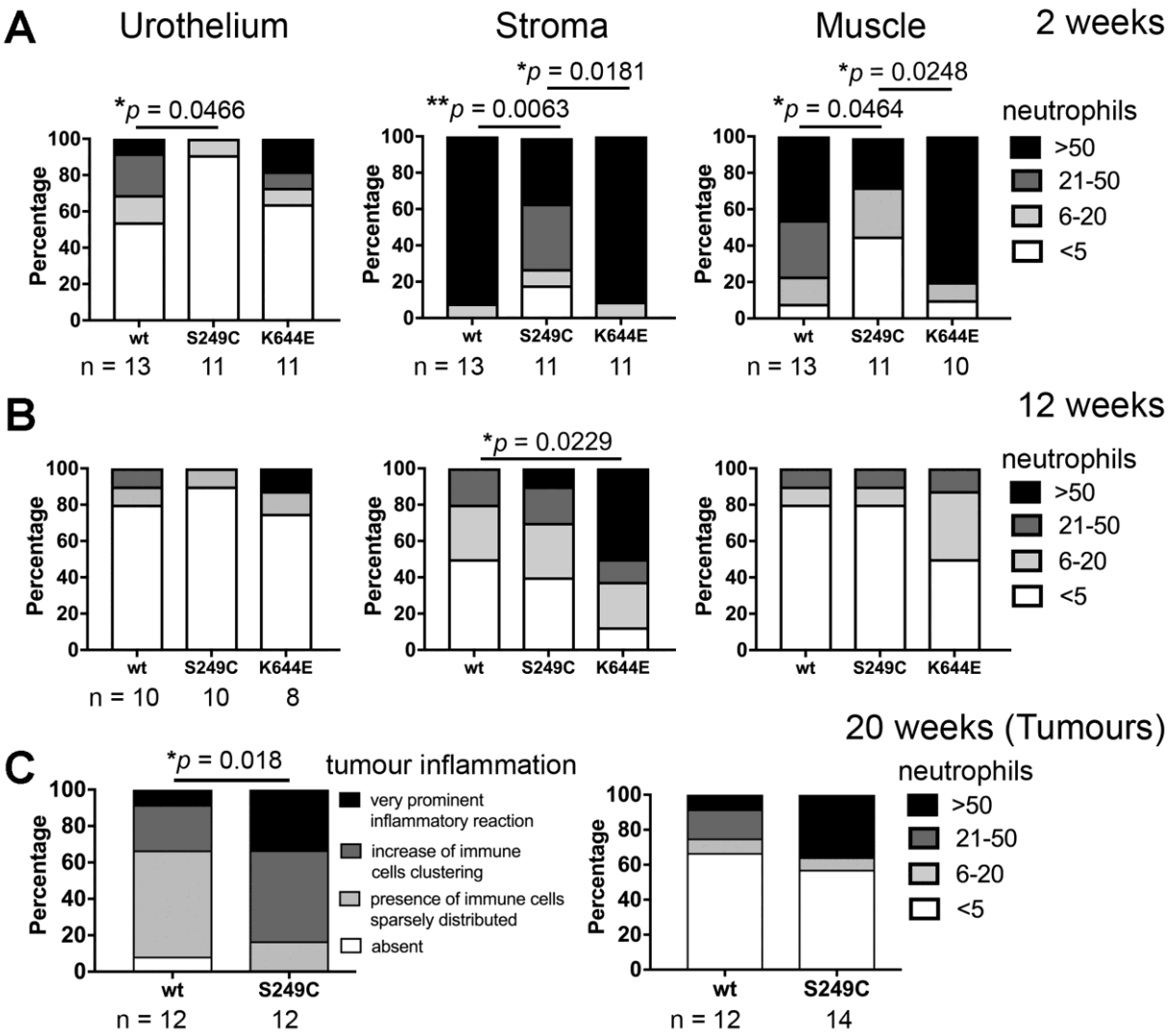

Figure 5. Depletion of Ly-6G$^+$ neutrophils to suppress OH-BBN induced inflammation in the bladder

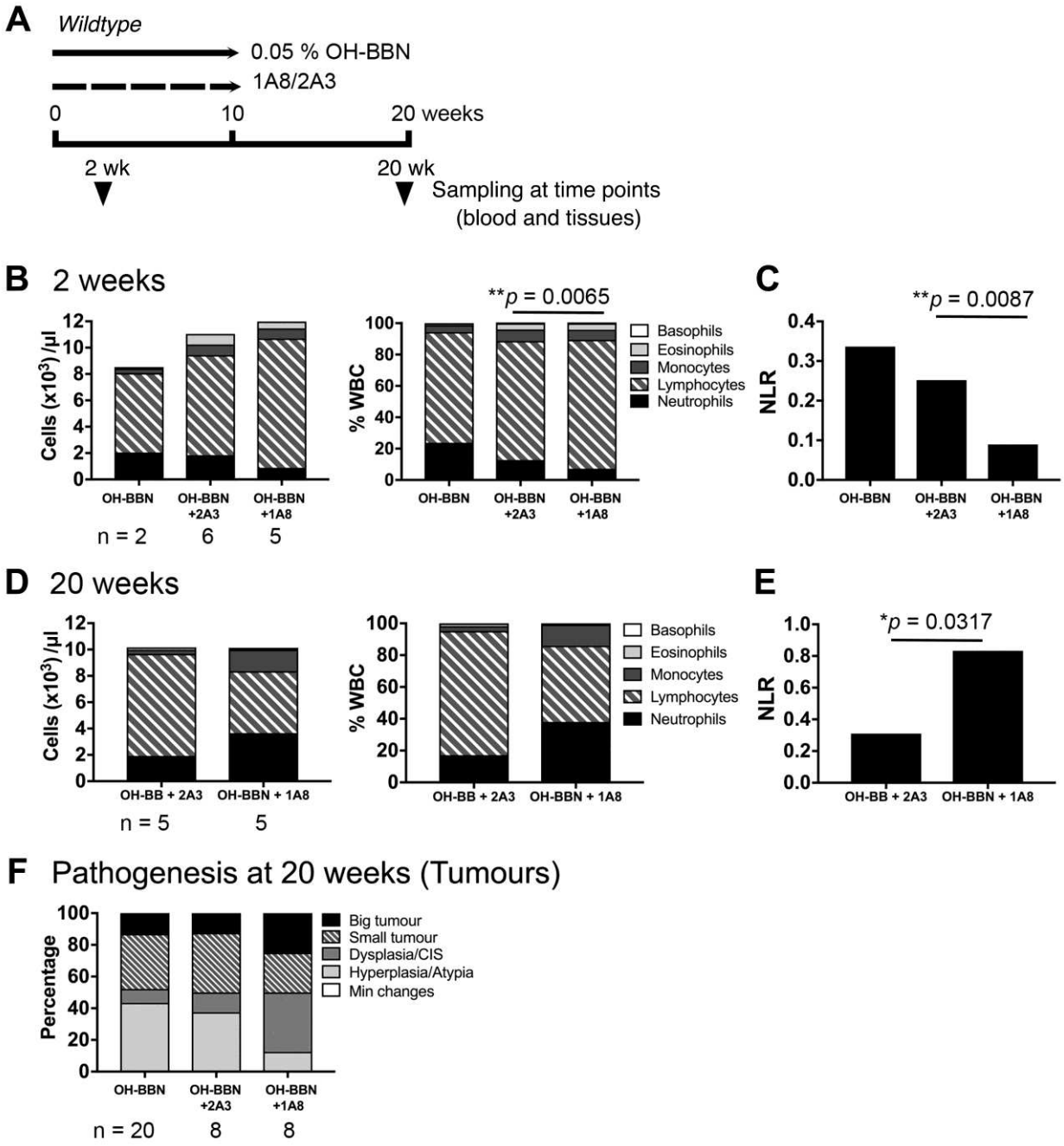

(**A**) Schematic presentation of the experiment. A monoclonal antibody against Ly-6G (1A8), was administered to mice during OH-BBN treatment for 10 weeks. Clone 2A3 was used as an isotype control. The composition of the white blood cells was analysed at 2 weeks (**B, C**), and at 20 weeks (**D, E**) from the start of OH-BBN treatment. Each leukocyte subtype was presented as a proportion within the total white blood cell population (% WBC). (**C, E**) Neutrophil-to-

lymphocyte ratio (NLR). (**F**) Pathogenesis in the bladder at the endpoint, shown as percentage of mice with the specific phenotypic criterion. Number of samples analysed is indicated below each column. The p-values (Mann-Whitney) are indicated where significant (*<0.05 and **< 0.005).

Figure 6: Proposed model of the mechanism underlying increased tumour development in the presence of an FGFR3 S249C mutation. Carcinogen induces DNA damage in the urothelium as well as an inflammatory response in the bladder that recruits neutrophils to the sites of damage. The balance between DNA damage and clearance of cells that harbour oncogenic mutations by inflammatory response determines the occurrence of the tumour and its pathogenesis. In $FGFR3^{S249C}$, reduced inflammatory response at early stages may impair the clearance of DNA-damaged cells, leading to increased tumour formation and severity at later stage. Enhanced tumour pathology may accompany perturbation of tumour inflammation. Early-phase depletion of neutrophils during tumour initiation led to increased circulatory inflammation at a later stage, indicative of enhanced tumour pathogenesis, which supports that suppression of acute inflammation could play a causative role in tumour pathogenesis.

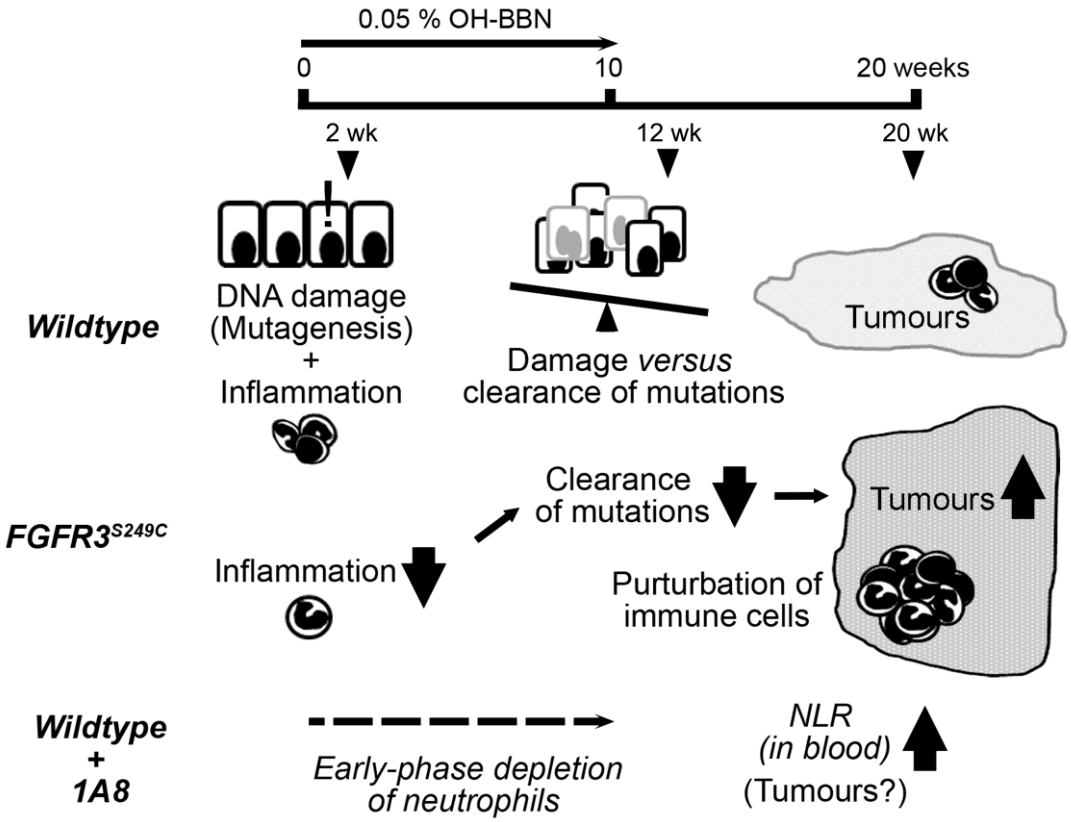

SUPPLEMENTARY MATERIAL ONLINE

Supplementary materials and methods YES

Supplementary figure legends NO, because all legends are embedded within the Suppl Figure S1–S9 PDF

Figure S1. Urothelial appearance of mice with FGFR3 S249C mutation at 12 months

Figure S2. Histopathology of the urothelium and the bladder tumours at 20 weeks from the start of the carcinogen treatment

Figure S3. Histopathology of the bladder at 2 and 12 weeks from the start of the carcinogen treatment

Figure S4. Response to DNA-damaging effects of OH-BBN treatment

Figure S5. Inflammatory characteristics of the bladder at 2 weeks of carcinogen treatment

Figure S6. Presence of the neutrophils in the bladder at 12 weeks of carcinogen treatment

Figure S7. Inflammatory phenotype of the bladder at 20 weeks from the start of application of carcinogen

Figure S8. Presence of neutrophils in the bladder tissues upon neutrophil depletion

Figure S9. Immune signature expression in TCGA datasets comparing FGFR3 mutant and Wildtype stratified by Lund or TCGA molecular subtype

Table S1. Summary of phenotype compared by gender

Table S2. Correlation of inflammatory phenotype by cohort and by bladder phenotype at 2 weeks

Table S3. Correlation of inflammatory phenotype by cohort and by bladder phenotype at 12 weeks

Table S4. Correlation of inflammatory phenotype by cohort and by tumour phenotype at 20 weeks